7-7-2015

Astrocytic Expansion in a Model of Neurofibromatosis 1 (NF1) Deficiency

Joel Rosiene
University of Connecticut, joel.rosiene@uconn.edu

Astrocytic Expansion in a Model of Neurofibromatosis 1 (NF1) Deficiency

Joel Rosiene

B.S., University of Connecticut, 2014

A Thesis Submitted in Partial Fulfillment of the Requirements for the Degree of Master of Science at the University of Connecticut

2015

APPROVAL PAGE

Master of Science Thesis

Astrocytic Expansion in a Model of Neurofibromatosis 1 (NF1) Deficiency

Presented by

Joel Rosiene, B.S.

Major Advisor: _____

Joseph J. LoTurco, Ph.D.

Associate Advisor: _____

Anastasios Tzingounis, Ph.D.

Associate Advisor: _____

Daniel Mulkey, Ph.D.

University of Connecticut

2015

Acknowledgements

It is first necessary to thank those individuals who have contributed in a multitude of ways towards the completion of this work. Principally, I should thank my major advisor, Dr. Joseph LoTurco, for graciously welcoming me into his lab and providing a great deal of mentorship and motivation during the course of this project. Additionally, students associated with the lab, both past and present, for being available as scientific resources and providing valuable and necessary input and expertise. Finally, I should thank profusely my friends and family for providing support and encouragement during the course of my studies, and for providing valuable feedback regarding the completion of this document.

Table of Contents

Abstract

Neurofibramatosis type 1 is an autosomal dominant disorder characterized by the development of both benign and malignant neoplasms of glial origin, as well as learning deficits and, less frequently, macrocephaly. Essential to the understanding of NF1 is the observation that the peripheral neoplasms (neurofibroma) which develop are composed primarily of NF1 negative glia which have undergone a loss of NF1 heterozygosity. The etiology of this loss of heterozygosity remains unclear, but a better characterization of these mutation events would provide insight into the cellular origins of the NF1 phenotype. CRISPR/Cas9 systems for genome editing have been, since 2013, a significant technique of interest by which precise mutagenesis may be achieved. Here we demonstrate a use of this system in conjunction with a Piggybac transposon lineage labelling approach by which the clonal identity of modified cell populations and the influence on cortical phenotype of a CRISPR/Cas9 induced model of NF1 deficiency may be investigated. Characterization of the induced NF1 phenotype is performed, and the CRISPR/Cas9 system is shown to be an effective method by which loss of cellular heterozygosity by somatic mutation may be modelled, exhibiting a monoallelic mutation rate of between 42.2% and 48.5. NF1 condition glia are not found to exhibit abnormal proliferation in the adult brain, and evidence supporting a model of neural progenitor fate switching to a glial phenotype in the form of CAG-TDTomato positive astrocyte populations derived from neuronal precursors is presented.

Introduction

Neurofibromatosis Type I

Neurofibromatosis type I is an autosomal dominant disorder with a prevalence in the general population of approximately 1 in 3,000, making it one of the most common mendelian neurodevelopmental disorders. The diagnostic symptom of NF1 pathology is the development of numerous neurofibromas throughout the central and peripheral nervous systems. These small tumors are composed of astrocytes (schwann cells in the periphery), mast cells, and fibroblasts. Neurofibromas that develop following loss of NF1 function in tumorigenic cells are categorized as being cutaneous, intraneural, or plexiform, with the first presenting primarily as benign cutaneous neoplasms, and the following exhibiting growth along neural sheaths, with occasional development of malignancy and impingement and disruption of local neural tracts. Indeed, the most serious impacts of the disorder on quality of life arise from growth of neurofibromas which disrupt normal neural function, resulting in blindness, chronic pain, hearing loss (common in NF2 with the development of schwannoma), and hypothalamic disturbance. Cutaneous neurofibroma generation can have dramatic cosmetic consequences, with the development of café au lait spots and benign cutaneous neoplasms. These superficial growths are generally considered too numerous to warrant individual surgical removal, and as such tend to accumulate over the lifetime of the NF1 heterozygous individual (Sabatini, et al. 2015). An additional tumor type, massive soft tissue neurofibromas, can more rarely be observed. These massive neurofibromas generally exhibit an enlarged plexiform phenotype which has progressed along the neural sheaths of an extremity, and generally result in a disfiguring enlargement of the limb in which they develop. Malignant peripheral nerve sheath tumors (MPNSTs) can occasionally arise from preexisting plexiform or massive soft tissue neurofibromas, with sudden onset

symptoms derived from impingement on to previously unaffected neural tracts (Schaefer, et al. 2015). More recently, inflammatory gastrointestinal polyps have been reported in a small case study of juvenile NF1 patients (Brosens, et al. 2015). Although debate exists regarding the causative effects of NF1 deficiency on the development of these polyps as opposed to other preexisting somatic mutations, it remains a possibility that as yet unidentified categories of peripheral neoplasms or hyperplastic cellular populations may exist within the context of Neurofibromatosis.

In the central nervous system, NF1 pathology primarily presents with pilocytic astrocytoma of the optic pathway, and often hypothalamus. Progression of these tumors results in visual deficits, or precocious puberty in young children. Surgical intervention is typically considered in those cases where neurological deficits or endocrine dysregulation develop. In the context of the brain, increased astrocytic density within the cortex has been recorded, with an additionally increased frequency of the development of low grade astrocytoma in human patients (Gutmann, et al. 2013). Production of astrocytoma has not been replicated in NF1 heterozygous mice, suggesting that astrocytoma growth likely requires a loss of NF1 heterozygosity in tumor progenitors which only occurs appreciably over longer time scales.

Molecular Characteristics of NF1

Recently, the molecular characteristics of the Neurofibromin protein have been better characterized. Analysis of the functional domains of the protein have established neurofibromin as a GTPase activating protein (GAP) which regulates the RAS protein pathway by promoting dephosphorylation of RAS-coupled GTP to GDP, which represents an inactivation of all downstream RAS effector pathways, including RAS-MapK, and RAS-Mek-ERK, which enhance cellular hyperplasia and proliferation, among other transcriptional effects (Ratner, et al.

2015) The observation that Neurofibromin acts primarily as a tumor suppressor via RAS coupled pathways has firmly placed NF1 disease in the realm of RASopathies, among others such as Noonan syndrome, Costello syndrome, and Canale-Smith syndrome (Brossier, et al. 2015). Despite this better understanding of the molecular interactions of Neurofibromin, the causes of the loss of NF1 heterozygosity, as is the case with many other tumor suppressors, remain unclear. Additionally, because NF1 is normally primarily expressed in neuronal populations in adult mice, the reasons for the cell-type specificity of proliferating populations in NF1 knockout conditions require more investigation (Bajenaru, et al. 2001). .

Heterogeneity among tumor cell populations has been observed in Neurofibromatosis related peripheral nervous sheath tumors, as well as other tumor disorders of the central and peripheral nervous systems (Yeh, et al. 2009). A significant degree of heterogeneity has, in fact, been associated with the most severe varieties of cancers, including glioblastoma, myeloid leukaemias, and colorectal cancers (Meacham, et al. 2013). Interestingly, established knowledge indicates that loss of NF1 heterozygosity in astrocytes and schwann cells alone is sufficient for the development of neurofibroma, as sequence data from NF1-associated neurofibroma has determined that only schwann cells among all of the cell types present in NF1-associated PNSTs were homozygous for nonfunctional NF1 (Kluwe, et al. 1999). Despite this evidence that malfunctioning astrocytes/schwann cells are primarily responsible for the development of PNSTs, it remains unclear whether the loss of heterozygosity occurs primarily in mature astrocytes or in some precursor populations (Bajenaru, et al. 2002).

CRISPR/Cas9

In 2013, the type II CRISPR/Cas9 system was introduced as a precise method of achieving mutagenesis and directed homologous recombination at select genomic loci in

Saccharomyces cerevisiae. Discovered first as a bacterial defense against the incorporation of viral DNA and later validated in human 293FT and mouse cells, the adapted system utilizes codon-optimized Cas9 nuclease from Streptococcus pyogenes to induce double stranded breaks immediately adjacent to a protospacer adjacent motif (PAM) site, of sequence NGG (Mali, et al. 2013). The production of double-stranded breaks in the genome leads to frame-shift insertions of deletions via non-homologous end joining (NHEJ) mechanisms. Specificity of Cas9 nuclease targeting is achieved by the transcription of noncoding RNAs (tracrRNAs) with spacer sequences homologous to target regions in the genome (Cong, et al. 2013). The ease of use of this genome editing technique, as well as its potential for multiplex application via the transcription of multiple guide RNAs, has resulted in the rapid adoption of CRISPR/Cas9 as the tool of choice for genomic editing across many different biological systems.

In the neural context, CRISPR/Cas9 has been successfully applied both in culture and in vivo to knock down the expression of synaptic proteins, although penetrance of the knockdown varies widely, an effect generally attributed to the design of the gRNA (Incontro, et al. 2014) (Straub, et al. 2014). Transfection protocols reported to be compatible with the CRISPR technique in neural contexts include biolistic transfection, use of adeno-associated viral vectors, as well as various surgical approaches typically paired with electroporation. As to the latter, In Utero Electroporation as well the more recently described Iontoporation(IPO) protocols have proven to be effective in achieving transfection of post-mitotic cortical neurons (De la Rossa, et al. 2015). Surgical electroporation approaches such as IUE and IPO generally circumvent challenges posed by the construct size limitations of viral vectors. This advantage has synergized well with the development of CRISPR/Cas9 multiplex systems, as well as the use of CRISPR/Cas9 with other plasmids, such as the Piggybac transposase lineage tracing technique.

IUE and IPO approaches also exhibit experimental flexibility, in that it has been shown that the date of IUE surgery reliably and reproducibly determines the laminar cohort within the cortex to which the transfected cells will ultimately belong (LoTurco et al. 2009).

The Piggybac transposase system has been used to perform fate-mapping and tracking of IUE transfected cellular populations. PBase mediated transposition of cassettes coding for fluorescent proteins into TTAA-rich genomic regions provides an effective tracing mechanism by which transfected cells and their progeny may be labelled. Under this schema, the PBase enzyme "cuts and pastes" regions of the donor plasmid flanked by inverted terminal repeats (ITRs) out of the donor and into the genome. Expression of PBase under various cell type specific promotors such as GLAST, Nestin, or EGFR, provides the Piggybac transposase system with additional flexibility in the ability to label only the progeny of a particular subset of transfected progenitors (Siddiqi, et al. 2014). Combination of the Piggybac transposase system with multiple fluorescent transgenes (piggyback donor plasmids) provides a method by which the size and tissue occupancy of single-color positive cell populations provide a reference for the rate of proliferation of singular transfected cells and their progeny (Chen et al, 2012).

Previously, a mouse model of Glioblastoma Multiforme has been induced via piggybac mediated transgenesis of HRasV12 and AKT under a CAG promotor. Transgenesis of these same genes under GFAP or MBP altered the tumor pathology – presenting with tumors populated by varying ratios of astrocytes, neurons, and oligodendrocytes. This finding suggested that cell type specific expression of oncogenic factors can result in tumor heterogeneity in the neural context. Tumor development, differentiation of component cellular populations, and ultimate pathological presentation are all altered by the characteristics of the cells of origin (Chen, et al. 2014).

Further investigation of this tumor heterogeneity, in combination with the lineage trace provided by the Piggybac system, and reliable mutagenesis drawn from the application of CRISPR/Cas9 has led to the development of a multiplex CRISPR/Cas9 system targeting three proto-oncogenic factors, the deletion of which also results in Glioblastoma Multiforme. In this system, CRISPR/Cas9 constructs targeting PTEN, NF1, and P53 were used to induce indel mutations in early exons of these genes, resulting in frame-shift loss of function. Alone, NF1 or PTEN CRISPR mediated knockdowns were sufficient to induce single-knockdown phenotypes. Specifically, the NF1 knockdown condition evidenced abnormal glial proliferation as evidenced by cells of astrocytic morphology spread across many cortical layers and present in abnormal densities. PTEN CRISPR condition brains, although lacking in any sort of laminar pathology or proliferative abnormality, presented with hypertrophic cortical neurons which evidenced lesser input resistance and increased spontaneous EPSC frequency when compared to controls. In particular, the lack clonal expansions (but with glial proliferation nonetheless) observed in the NF1 condition, along with the relevance of the NF1 phenotype to clinical observations marked this as an avenue of further study into the nature of the NF1 phenotype and the use of the CRISPR/Cas9 system to induce models of neuroglial disorders.

Glial disorders in general are fairly common throughout the population, and present with diverse pathologies, often involving damage to neurons secondary to either a proliferation or a degeneration of glial cells. Multiple sclerosis, a characteristic disease involving microglial activation and corresponding inflammation, affects globally approximately 30 people in 100,000. MS typically involves an inflammation mediated degeneration of myelinated axons in the affected area, with neurological deficits arising in accordance with the regions of the central nervous system affected. Defects in visual ability, motor coordination, vestibular sense, and

cognition are all common symptoms (Fields 2010). In the context of other disease phenotypes, dysfunction of the glia have been implicated in a variety of neurological disorders including Neuromylitis optica, and Amyotrophic Lateral Sclerosis, as well as, more generally, other TDP-43 positive neuropathologies (Sloan et al 2013). Astrocytes in particular have been suggested recently to modify synaptic function via 5-HT2B mediated changes in protein expression, and thereby participate in mood-affecting modulation of serotonergic synapses (Zhang, et al. 2010). Finally, work with mouse models of Rett syndrome suggests that MeCP2 deficient astrocytes exhibit abnormal patterns of mRNA expression which are sufficient to produce abnormal changes dendritic morphology in vitro (Ballas, et al 2009).

Because of the remaining questions associated with the nature of NF1-induced astrocytoma and PNST, it seemed appropriate to use developing technology (CRISPR/Cas9) to produce a murine model of NF1 heterogeneity. Specifically, the use of In Utero Electroporation combined with point-specific mutagenesis provided by the CRISPR/Cas9 system has allowed for the production of a marked NF1 CNS phenotype without the need for production of a traditional NF1 heterozygous animal. The nature of the IUE CRISPR/Cas9 approach also provides that the behavior of a small percentage of heterozygous and knockout cells within the context of an otherwise wild type brain may be characterized and better understood. Clearly, the knockout and subsequent observation of only particular developing cell lineages better represents the multi-step model of tumorigenesis as compared to global or even cell type specific knockouts. The production of the rat CRISPR/Cas9 induced NF1 model also provided for both an evaluation of the function of the IUE CRISPR/Cas9 system, as well as for characterization of the proliferative markers present in adult NF1-phenotype cortex and the identity of NF1 knockout induced glial proliferations in the cortex. Of particular interest was the question – do increased astrocyte

counts in NF1 cortex occur as a result of clonal expansion (as they do in similar models of aggressive glioblastoma), or are these changes better represented by a model involving large scale upregulations in proliferation and differentiation of astrocytic precursors?

Methods:

Cloning for Px330 vectors:

Short guide RNA oligos were designed via the use of an online tool from crispr.mit.edu against exonic sequences from PTEN, P53, and NF1 genes in the rat genome. CACC and AAAC 5' tails were added to the complementary oligos to provide for BbsI digest mediated ligation into Px330 vectors. Guide sequences used for PTEN were 5'-ATTTGGAGAGAAGTATCGGT-3' (forward) and 5'-ACCGATACTTCT CTCCAA AT -3' (reverse). Guide sequences for P53 targeting were 5'- CTTCCACCCGGATAAGATGT-3' (forward) and 5'-ACATCTTATCCGGGT GGA AGC -3' (reverse). Guide sequences for NF1 targeting were 5'-GGTCAGCCGCTTCGACGAGC-3' (forward) and 5'-GCTCGTCGAAGCGGCTGACC -3' (reverse). All oligos were ligated into the BbsI digested linearized Px330, gel purified, and sequence verified.

Animal Care

All animals used were pregnant Wistar rats sourced from Charles River Laboratories, Inc (Wilmington, MA). Animals were received and cared for at the University of Connecticut PBB Vivarium on a 12 hour day/night cycle and fed ad libitum, with water provided via water bottle. Embyronic day of embryonic pups was estimated via palpation, with mothers sedated via Isoflurane. Day to day animal care was provided by PBB Vivarium staff, and all procedures were approved by the Institutional Animal Care and Use Committee at the University of Connecticut.

Plasmid Preparation for IUE

Plasmids were prepared for IUE injection to a final concentration of 1ug/ul via speedvac or ethanol precipitation. Fast green was added to the mixture to a final concentration of 0.5% to allow for visualization of the injection site.

In Utero Electroporation

All animal procedures detailed in this section were performed to the standard of approval set by the Institutional Animal Care and Use Committee of the University of Connecticut. Pregnant females were anesthetized for surgery via subcutaneous injection of 100mg/kg ketamine and 7mg/kg xylazine following light anesthetization via Isoflurane. A 1cm (approximate) incision was then made through the dermal layers, subdermal fascia, and muscle layer along the midline of the lower abdomen. Uterine horns were visualized and removed gently from the abdomen, and constantly hydrated via application of PenStrep saline. In Utero transfection of embryonic day 14 or 15 animals was achieved by ventricular injection of approximately 1ul of plasmid mixture through glass capillary needle powered via Picosprizter (Parker Hannifin). Electroporation was performed using a BTX ECM 830 electroporator set to provide five sequential square pulses of 65 V, in 50msec durations. Following electroporation, the uterus was returned to its original position in the abdomen, and incisions were closed in two layers using 4-0 nylon suture.

Data Collection and Immunohistochemistry

Pups gained from IUE procedures were raised to postnatal day 21, at which point they were sacrificed. Transcardial perfusion was performed after first deeply anesthetizing the animal with Isoflurane. Adult rats were perfused first with 20ml of PBS followed by 20ml 4% w/v

PFA. Brains were removed immediately following transcardial perfusion and fixed overnight in 4% PFA. Sectioning was performed on a Leica VT 1000S vibratome at a uniform 65 um thickness.

Antigen retrieval was performed when P53, NF1, and PTEN antibodies were used. Tissue sections were incubated at 95 C in 10mM Sodium Citrate.

Primary antibody incubations were performed over 36 hours with PTEN (Cell Signaling, 9559), NF1 (Santa Cruz, 67), P53 (Cell Signaling 2982) antibodies. Fluorescence images were acquired using a Zeiss Axio imager M2 microscope with Apotome with 488/546/350 nm filter cubes and the X-Cite series 120Q light source. Further image processing and color channel separation was performed using ImageJ.

Imaging Protocol

For the purposes of CRISPR efficiency quantification, all images were obtained using a 20x objective (40x for representative images). Transfected neurons in each section were counted and evaluated for NF1, PTEN, or P53 antibody signal. Image stacks used for quantification were acquired only through Z-sections of the tissue that showed antibody signal.

For quantifications of astrocyte to neuron ratio, acquired images consisted of maximum projection stacks of cortical columns, from the pial surface to the white matter, within transfected regions of tissue. S100B positivity was used to provide definitive identity of astrocytes, while morphology and NeuN positivity were used as neuronal markers.

Surveyor Assay and Fluorescence Activated Cell Sorting

In Vivo SURVEYOR assay was performed on genomic DNA obtained from dissected tumor samples via Blood and Tissue DNA easy kit (Qiagen). Genomic regions containing

CRISPR targetsites were PCR amplified and SUVEYOR assay was performed using a SURVEYOR assay kit (IDT 706025) according to manufacturer's instruction. Primers for SURVEYOR assays are: PTEN exon 6 Forward: CATCCATGTGAGGAACCCTGGGTG; PTEN exon 6 Reverse: CACTTACTG CAAGTTCCGCC; PTEN exon 8 Forward: CCACAAGGTGTTTGCCTTCA; PTEN exon 8 Reverse: CTCGAGATCCAAAGGCATTG; NF1 exon 1 Forward: GACGTCACCTCCAGGAGGAC; NF1 exon 1 Reverse: TGGGATAAAGGGGATGGAGGG; P53 exon 6 Forward: CCCACTTTGACCCTTGATCC; P53 exon 6 Reverse: CAGGCACAAACACGAACCTC.

Fluorescence Activated Cell Sorting of tumor material was performed to enrich for CRISPR/Cas9 induced mutations. Animals were deeply anesthetized with Isoflurane and decapitated. Dissection of fluorescent brain regions (tumor) was performed cold in PBS under a fluorescent dissecting scope. Dissociation of the dissected tissue was performed via 10 minute incubation at 34 degrees Celsius with Proteinase XXXIII Asergillus (Sigma P4032). Proteinase reaction was halted using one equal volume Trypsin inhibitor at 1mg/1mL concentration (Sigma T9253). Tissue chunks were triturated through a series of Pasteur pipettes of decreasing aperture size until a uniform cloudy suspension was produced. Finally, the cell suspension was passed through 70um followed by 40um mesh filters prior to FACS.

Genetic material was recovered from FACS samples via application of a QIAGEN Blood and Tissue kit. Genomic PCR was performed using the same primers as described in the SURVEYOR assay protocol. Amplified regions were cloned into TOPO_2.1 sequencing vector and sequenced using m13 primers.

	Px330-NF1	Px330-PTEN	Px330-P53	Px330-NF1, Px330-PTEN, Px330-P53	Px330-Tyr1 (Control)
Multicolor Piggybac GLAST-PBase				Ki67	Ki-67
PB-GFP, CAG-tdTomato, GLAST-PBase	S100B				S100B
Single Color Piggybac, GLAST-PBase	NF1 Ki-67	PTEN	P53		NF1 PTEN P53 Ki-67

Table 1: Summary of Experimental Groups and Antibody Probes.

Multiple combinations of both multiplexed CRISPR/Cas9 constructs as well as Piggybac and non-Piggybac fluorophores were transfected via IUE to produce the material presented in this work. A summative table showing the applied combinations of plasmids is presented above, with applied combinations darkened.

Results

IUE CRISPR/Cas9 procedures were performed to elict single and multiplex knockdown of PTEN, P53, and NF1 genomic targets. Triple transfected brains (PTEN,P53, and NF1) were cotransfected with either a three color (PB-GFP, PB-mRFP, PB-CFP) or a single color (PB-mRFP) plasmid system. PTEN single CRISPR/Cas9 transfections were labelled episomally with CAG-GFP, as were P53 single transfections. NF1 transfections were cotransfected either with PB-mRFP or with PB-GFP plus CAG-TDTomato, with the addition of GLAST-PBase. In addition to single and triple target conditions, combinations of two CRISPR/Cas9 factors were used to produce each possible double-knockdown condition. In all cases control brains labelled with the same fluorophores and cotransfected with stock Px330 (without guide RNA inserts) were used to provide a reference of wild type morphology.

NF1 Single Transfected Condition

As described above, transfection with a CRISPR/Cas9 contruct targeting exon 1 of the NF1 gene encoding for Neurofibromin resulted in a dramatic glial phenotype evident across the entire width and breadth of the transfected hemisphere. Glial proliferation was the most obvious morphological change in these conditions, with a corresponding decrease in the density of transfected neurons also becoming apparent after imaging and quantification. Lineage labelling data would suggest that most of the glial expansion is not clonal in nature, as single color clonal expansions as seen in the induced tumor conditions are not present in NF1 astrocyte populations.

P53 Single Transfected Condition

Interestingly, although P53 is well characterized as an important tumor suppressor, mutations of which are present in a great variety of human cancers, P53 CRISPR-mediated

knockdown alone did not evidence any gross pathological phenotype. A likely explanation for this observation derives from the two hit model for tumorigenesis, wherein multiple genetic insults to tumor suppressors are required for development of neoplasm. It is likely that in the murine context, one to two months of survival prior to sacrifice likely do not provide enough time for the development of these spontaneous mutations.

PTEN Single Transfected Condition

Animals transfected with CRISPR/Cas9 constructs against the PTEN gene evidenced neuronal hypertrophy and altered electrophysiology in transfected layer 2/3 neurons. PTEN is well characterized as an important negative regulator of the mTOR pathway of cellular proliferation. PTEN knockout animals did not evidence any glial phenotype such as in the NF1 condition, and neuron/astrocyte ratios in these animals remained unchanged from controls.

Triple Transfected Condition

Transfection of CRISPR/Cas9 constructs against all three tumor suppressor genes reliably resulted in the production of tumors as evidenced by greatly increased fluorescent cell density in the transfected hemisphere. Gross anatomical observation of the transfected brain also revealed a general enlargement of the transfected hemisphere observable as early as post-natal day 19. Sectioning and fluorescent imaging of these tumor brains revealed distinct cellular populations within the tumor as labelled by the multicolor Piggybac Transposon system. Regions of single color transfection against a diverse and multi-color background indicate regions of the tumor arising from a single transfected progenitor. Notably, clonal populations of transfected cells were observed occasionally in the hemisphere contralateral to the site of transfection, suggesting

that tumor cells produced via mutation of these three factors are highly malignant. Transfected cell populations in the contralateral hemisphere were never observed in the control condition.

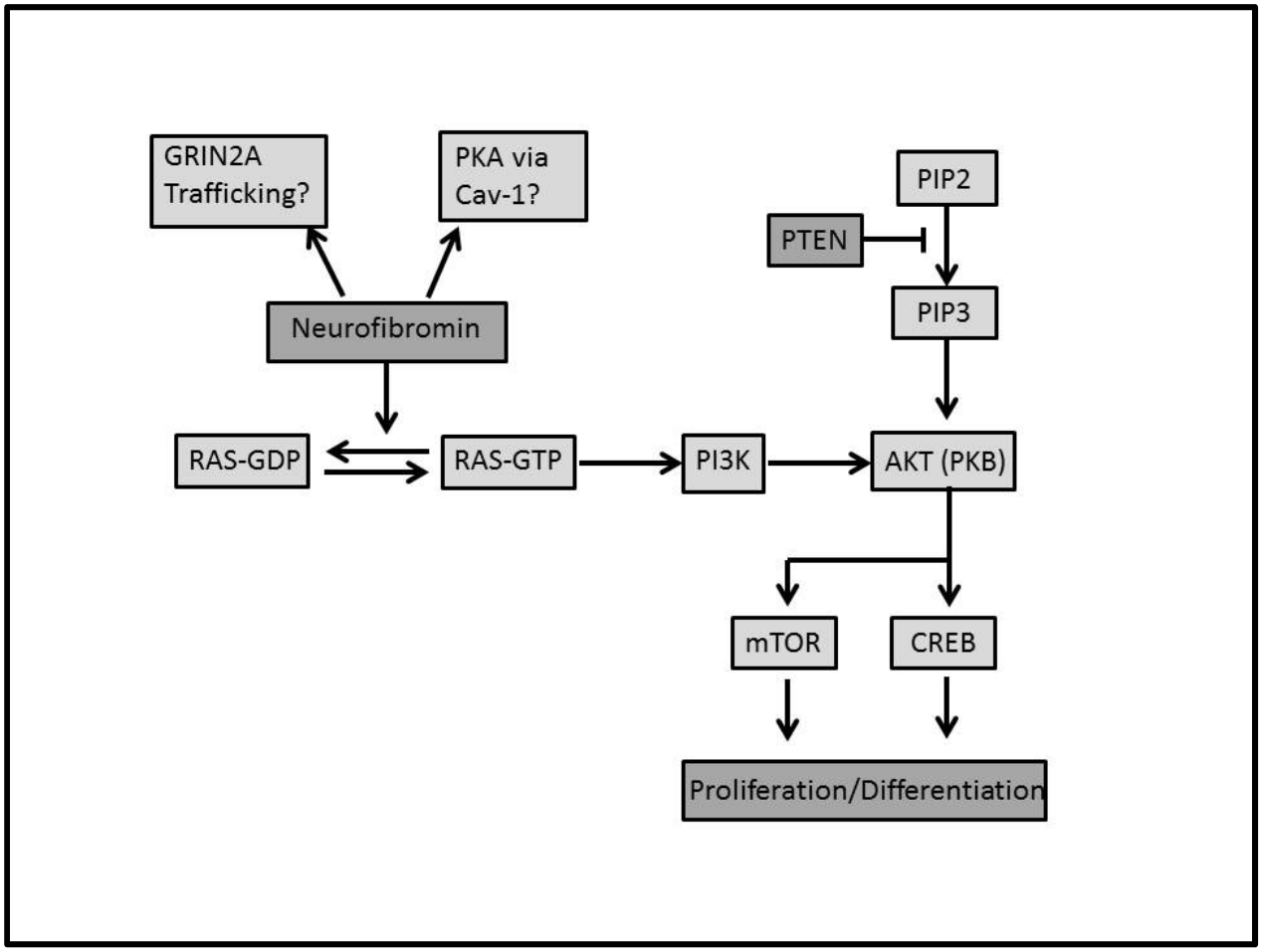

Figure 1: Established and putative roles for Neurofibromin and PTEN in the context of cellular proliferation.

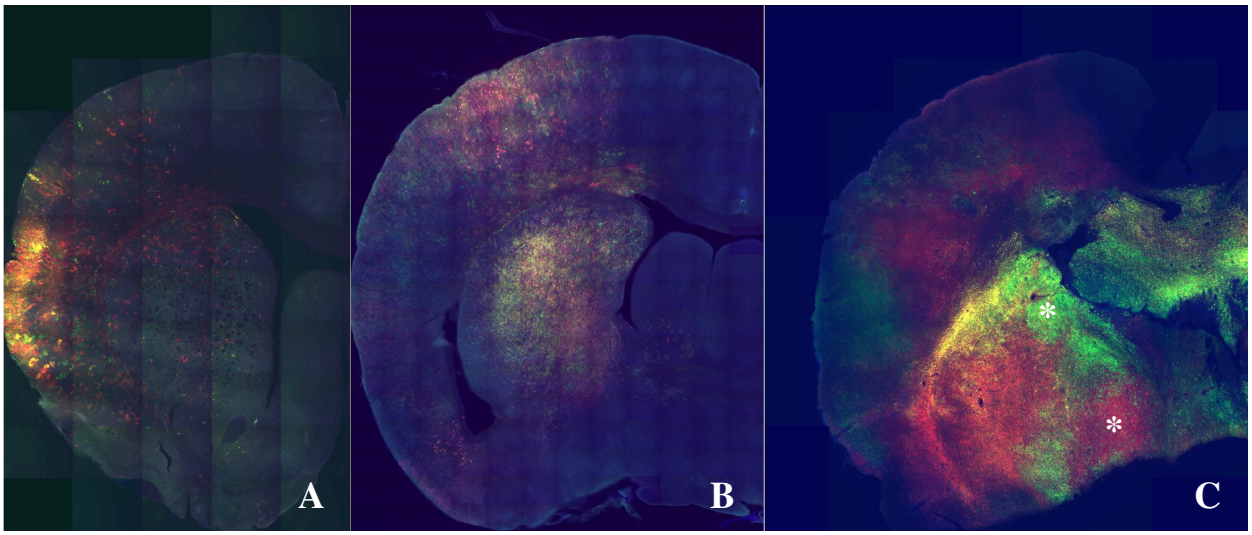

Figure 2: Multicolor Stitches

(A) Px330-Tyr1 Multicolor control brain with PB-GFP, PB-mRFP, and GLASTPBase. Astrocytic populations are labelled, but glial density is less than that of the Px-330 NF1 condition, and no single-color clonal populations are present.

(B) Px330-NF1 Multicolor transfected brain with PB-GFP, PB-mRFP, GLAST-PBase. Whole-hemisphere increase in glial density is evident, but there is a distinct lack of single-color clonal populations.

(C) Multicolor Tumor Brain Section transfected with Px330-NF1, Px330-PTEN, Px330-P53, and Piggybac transposon lineage labelling system (PB-GFP, PB-CFP, PB-mRFP, GLAST-PBase). A dense tumor core is visible, as are single color clonal expansions of cancerous cells arising from single progenitors. Asterisks indicate single color clonal regions.

Double Transfections

Cellular morphology and density in P53+NF1 and P53+PTEN knockdown conditions corresponded exactly to the phenotype already observed in the NF1 and PTEN conditions respectively. That is to say, the inclusion of CRISPR/Cas9 constructs against P53 for cotransfection with NF1 and PTEN targeting constructs neither added to nor detracted from features of the produced phenotype. NF1+PTEN transfection produced a phenotype with the full features of both the NF1 and PTEN conditions (glial proliferation and neuronal hypertrophy) to an extent greater than that of either single transfection, but histology was not performed to positively identify tumor pathology.

Quantification of Ki-67 positivity as a metric of active proliferation.

Ki-67 is well established as an antigen which reliably labels mitotic cells. As such, density of Ki-67 staining is useful as an indicator of the degree of cellular proliferation occurring in a tissue at the time of fixation. For the purposes of this experiment, postnatal day 19 animals were sacrificed and their brains stained with Ki-67. Only glial cells labelled with a GLAST-PBase/Piggybac fluorophore system were counted. The percentage of labelled glia that were Ki-67 positive in control sections was 0.84%, calculated across 355 glial cells. The percentage of labelled glia that were found to be Ki-67 positive in NF1 condition sections was 1.56%, calculated across 1564 glial cells.

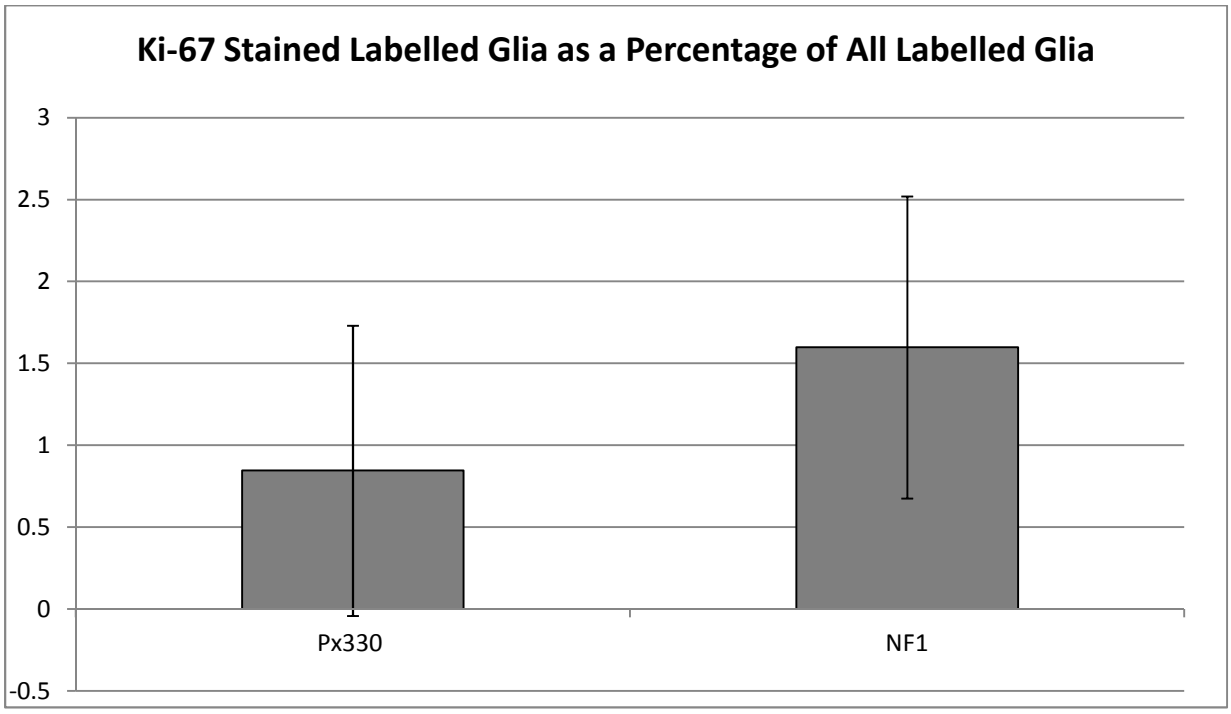

Figure 3: Ki-67 Quantification in Labelled Glia

Differences in Ki-67 positivity among glial cells between the Px330-NF1 experimental tissue and control brains were not significant. P=0.1644

Quantification of CRISPR Induced Knockout Efficiency

Immunohistochemistry staining against CRISPR/Cas9 targets in the transfected tissue was performed to gain a quantification of the rate of successful CRISPR induced knockdown. For these purposes, P53, PTEN, and NF1 negative neurons were counted as a fraction of all transfected neurons.

Swaths of transfected cortex were imaged at high resolution and analyzed for frequency of target-negative phenotypes in neuronal populations. Glial populations were not counted, as the E14 IUE transfection typically only results in neuronal transfection. Target-negative neurons were quantified as a percentage of all transfected neurons. In this case it is important to recall that negative expression in this case reflects biallelic loss of expression mutation, and may not reflect the majority of CRISPR/Cas9 induced mutation events. In the PTEN condition, of 381 neurons counted, 71 were negative for PTEN, a knockout frequency of 17.8%. In the PTEN Control condition, of 314 neurons counted, 5 were negative for PTEN, a knockout frequency of 1.2%. In the NF1 condition, of 564 neurons counted, 132 were negative for NF1, a knockout frequency of 21.6%. In the NF1 Control condition, of 514 neurons counted, 10 were negative for NF1, a knockout frequency of 1.75%. In the P53 condition, of 182 neurons counted, 43 were negative for P53, a knockout frequency of 23.5%. In the P53 Control condition, of 420 neurons counted, 4 were negative for P53, a knockout frequency of 0.9%.

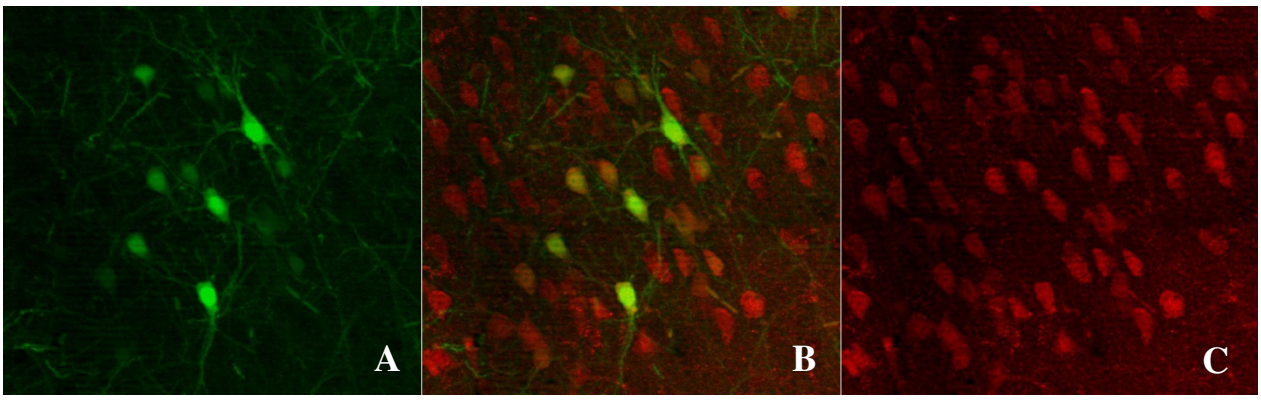

Figure 4: Px330 Control Section Stained against Neurofibromin. Px330 (without guide RNA insert) CAG-GFP labelled transfected layer 2/3 cortical neurons. (A) Normal neuronal morphology and density can be observed. (B) All GFP labelled neurons were positive for Neurofibromin. (C) Typical Neurofibromin expression in pyramidal neurons is present.

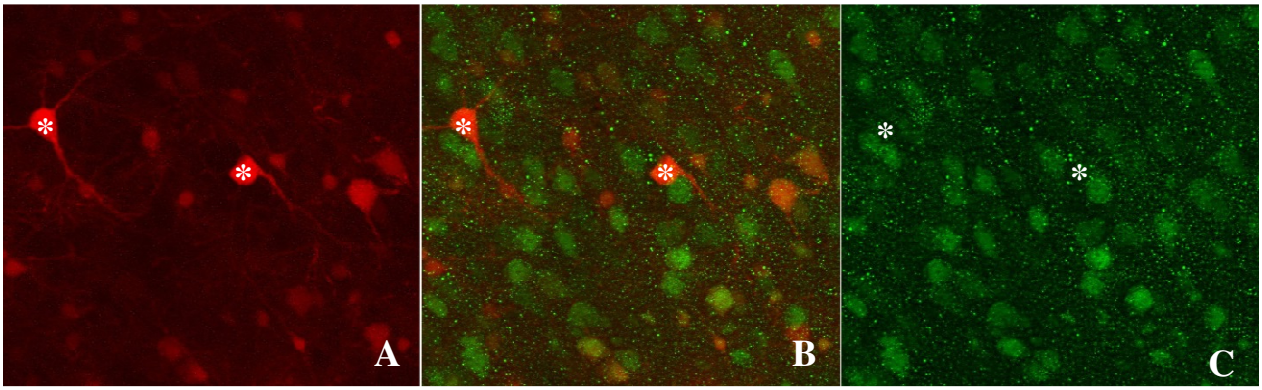

Figure 5: Px330-NF1 Transfected Section Stained against Neurofibromin. Px330-NF1 transfected (with NF1 guide RNA insert) PB-mRFP, GLAST-PBase labelled transfection in layer 2/3 cortical neurons and glia. Decreased neuronal density in layer 2/3 and increased glial density can be observed. (A) PB-mRFP labelled neurons and glia. (B) Representative labelled neurons negative for neurofibromin. (C) Neurofibromin staining. Asterisks indicate positions of NF1 negative neurons

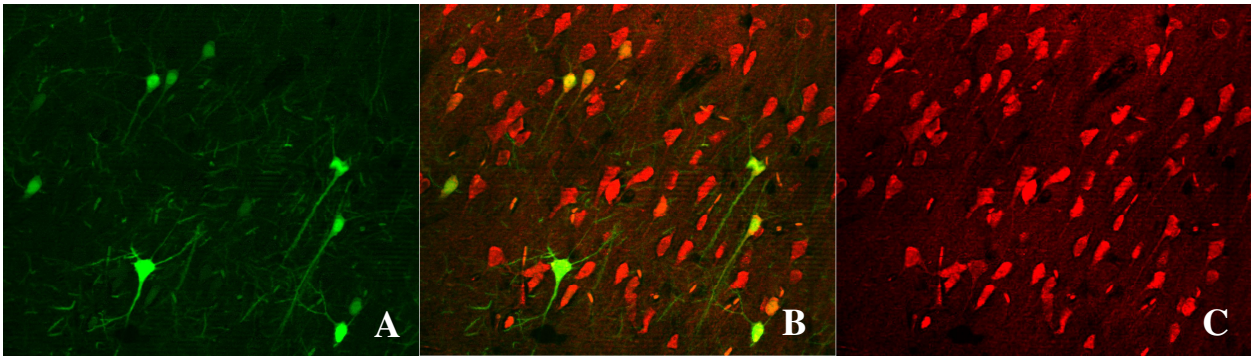

Figure 6: Px330 Control Section Stained against PTEN. Px330 (without guide RNA insert) CAG-GFP labelled transfected layer 2/3 cortical neurons. (A) Normal neuronal morphology and density can be observed. (B) All GFP labelled neurons were positive for PTEN. (C) Typical PTEN expression in pyramidal neurons is present.

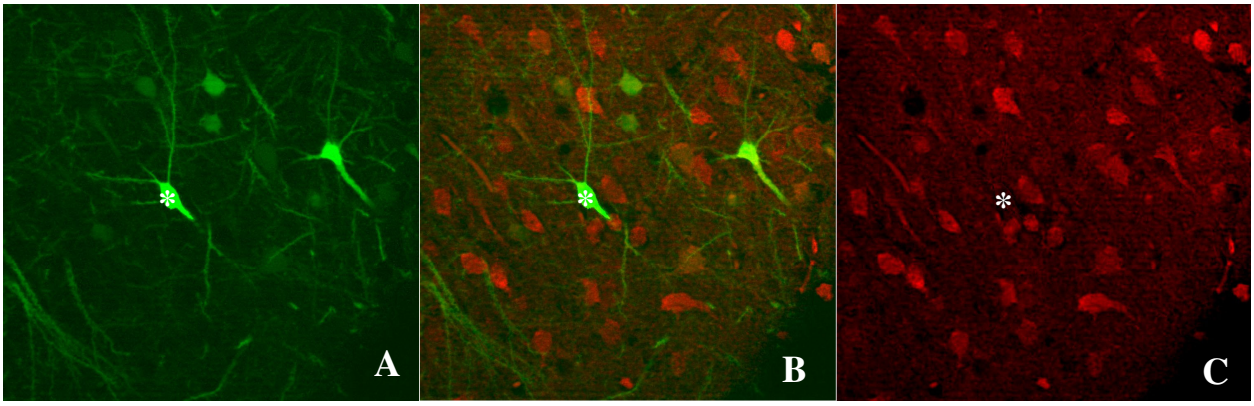

Figure 7: PX330-PTEN-E8 Section Stained Against PTEN. Px330-PTEN-E8 transfected, CAG-GFP labelled layer 2/3 neurons. (A) CAG-GFP labelling in layer 2/3 neurons. (B) Representative image shows CRISPR-induced PTEN negative neuron. (C) PTEN staining. Asterisk indicates PTEN negative neuron.

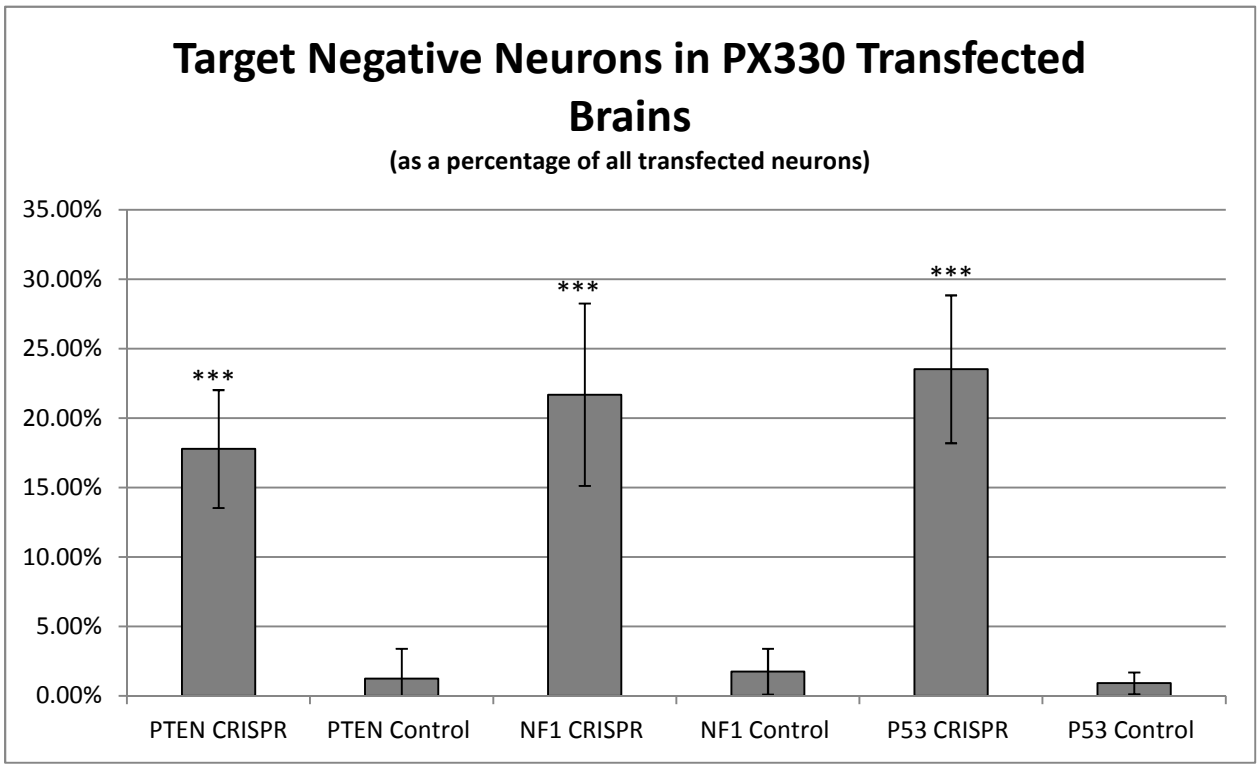

Figure 8: Efficiency of CRISPR Induced Mutation as Quantified by IHC Bar graph showing fractional percentage of CRISPR target knockout in transfected neurons. Across the three conditions, the CRISPR/Cas9 system evidenced a full knockout rate of between 17.7% and 23.5%. Monoallelic mutation events and mutations that did not lead to loss of antibody-targeting epitopes are not represented. Presented standard deviation was calculated across knockout/transfected ratios on a per brain basis. P value for PTEN = 1.61E-6. P value for NF1 = 8.78E-6. P value for P53 = 9.86E-5.

Quantification of Astrocyte/Neuron Ratios across All Experimental Conditions

Cortical columns were imaged across all experimental conditions (PTEN, P53, and NF1), as well as PX330 control in brains labelled with GLAST-PBase and a Piggybac-fluorophore (either PB-mRFP or PB-GFP). Sections were stained for S100B, an astrocytic marker, and transfected cells positive for S100B were quantified in addition to transfected neurons. The ratio of labelled astrocytes to neurons in the PTEN condition was 0.16, across 449 cells counted. The ratio of labelled astrocytes to neurons in the NF1 condition was 5.66, across 974 cells counted. The ratio of labelled astrocytes to neurons in the P53 condition was 0.34, across 215 cells counted. Control Px330 brains possessed an astrocyte to neuron ratio of 0.81, across 1382 cells counted. Raw density of astrocytes and neurons within the cortical columns quantified was recorded, but was found to be highly variable and is not reported.

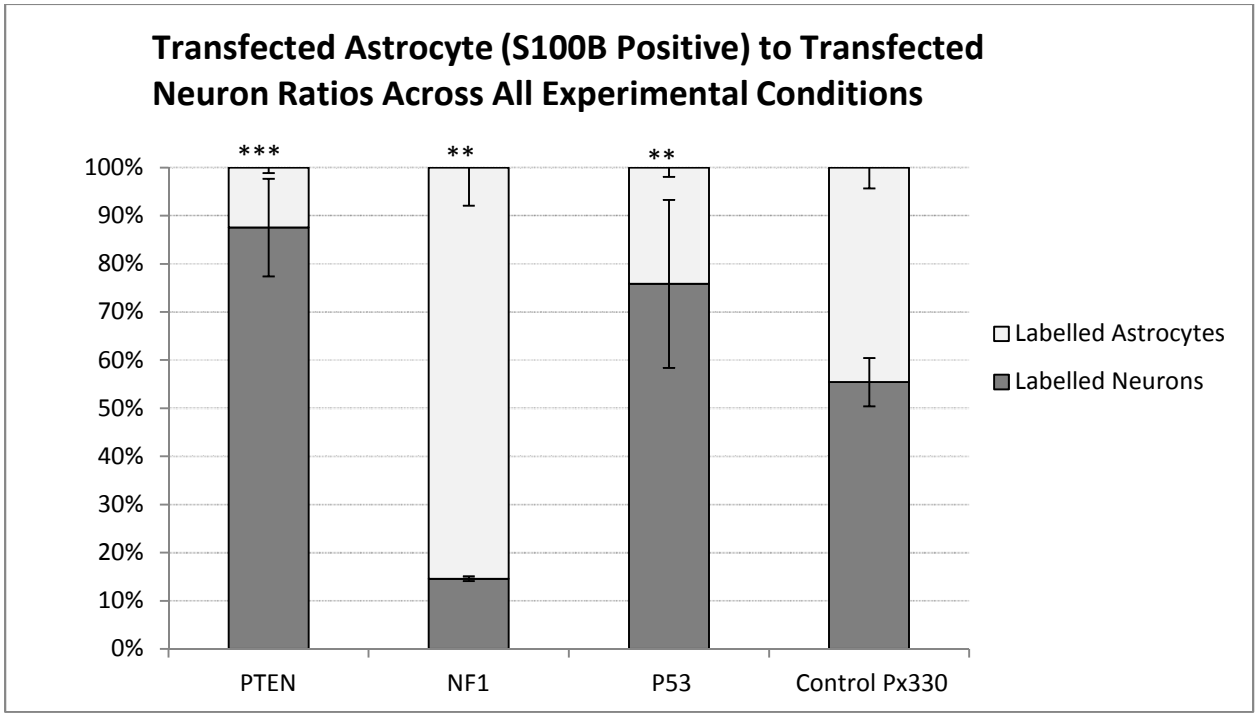

Figure 9: Quantification of S100B Positive Labelled Glia and Labelled Neurons. Px330-NF1 transfected brains present with greatly elevated astrocyte to neuron ratios when compared to PTEN, P53, and control Px330 conditions. Different brains within the NF1 condition evidenced a range of astrocyte/neuron ratios between 3.15 and 7.58, but these ratios were invariably significantly elevated when compared to controls. P value for PTEN = 4.10E-4. P value for NF1 = 4.06E-3. P value for P53 = 1.41E-3

Observation of Astrocytic CAG-TDTomato Positive Populations in the NF1 Condition

In GLAST-PBase PB-GFP CAG-TDTomato Px330-NF1 transfected brains, groupings of TDTomato positive astrocytes were observed at various layers within the cortex. These groups of astrocytes were composed of between 5 and 30 cells, and all cells were PB-GFP positive. In E14 IUE brains, CAG-TDTomato labelling would typically only be restricted to birthdated neurons, as episomal plasmids tend to be diluted under conditions of heavy proliferation. Indeed, no TDTomato positive astrocytic populations were found in control brains. S100B positivity was evaluated to establish astrocytic identity of these TDTomato positive populations.

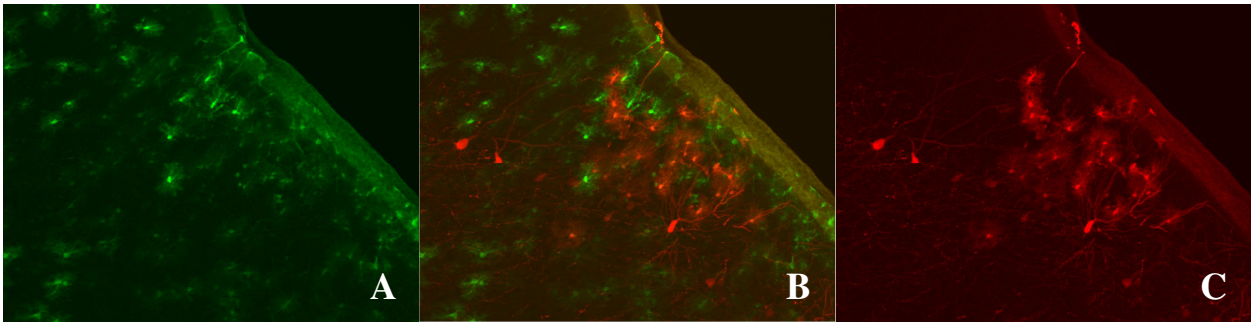

Figure 10: Px330-NF1 Condition Brain CAG-TDTomato labelled populations of astrocytes are found in Px330-NF1 tissue labelled with CAG-TDTomato, PB-GFP, GLAST-PBase. (A) PB-GFP labelling of astrocytes. (B) CAG-TDTomato positive groups of astrocytes are all PB-GFP positive. (C) CAG-TDTomato positive groupings of astrocytes are present.

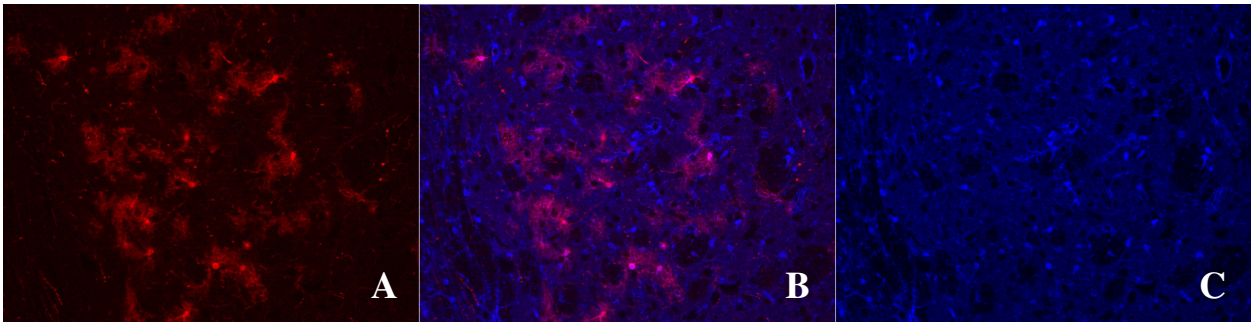

Figure 11: Astrocytic CAG-TDTomato populations in Px330-NF1 Condition Brain. CAG-TDTomato positive groupings of cells were established to be astrocytes via S100B staining in brain transfected with Px-330-NF1, CAG-TDTomato, PB-GFP, GLAST-PBase. All TDTomato positive cells in frame are S100B positive. (A) CAG-TDTomato labelling of astrocyte group. (B) All CAG-TDTomato positive cells were also S100B positive. (C) S100B staining.

Discussion

Proliferation of NF1 Condition Glia in Adult Brain

Ki-67 positivity of labelled glia in the NF1 condition was not found to be significantly higher than controls. This observation, in combination with the well characterized increase in glial density in the same tissue, would suggest that said increase derives not from a persistent up regulation of cellular proliferation, but from another event earlier in development. Such an event could be either a transient increase in the proliferative rates of glial precursors, or a fate change by which neuronal progenitors become glial progenitors, inflating the size of the ultimate glial population.

Efficiency of the IUE-CRISPR/Cas9 system

Across the three tested conditions, the efficiency of the IUE-CRISPR/Cas9 in achieving biallelic loss of function mutation in transfected neurons ranged from 17.8% (in the PTEN condition) to 23.5% (in the P53 condition). The NF1 condition presented with a 21.6% knockout rate. This particular data point should be regarded as a low estimate of efficiency, as fate-switching of induced NF1-negative progenitors away from ultimate neuronal fates would influence any neuron based quantification. As the completed quantification provides a measure of biallelic knockdown, theoretical monoallelic mutation frequencies can be calculated. Theoretical monoallelic mutation frequencies for the three conditions are thus – PTEN – 42.2%, NF1 – 46.5%, and P53 – 48.5%. The variation present in these mutation rates may be derived from a range of factors which may affect CRISPR/Cas9 efficiency, including but not limited to; guide RNA affinity, expression levels of the CRISPR/Cas9 construct, and the chromatin state of the genomic target.

Evidence for the Development of NF1 Phenotype via Fate Switching

The lack of single color clonal populations in the NF1 phenotype would indicate that the increased glial density observed in this condition does not come about as the result of the proliferation of tumor stem cell-like modified progenitors. Instead, it is clear from observations of CAG-TDTomato positive astrocytic populations present in E14 transfected brains that at least some of the astrocytes present in our model of NF1 phenotype cortex are derived from transfected neural progenitors originally slated to become cortical neurons. While this explanation cannot account for the entirety of the increase in glial density (indeed, only a lesser percentage of glia in these brains are TDTomato positive), this data would suggest at least that CRISPR/Cas9 induced loss of NF1 drives neural progenitors away from the typical neural fate.

Presence of pCAG-TDTomato positive astrocytic populations within layers 2/3 of the rat cortex in the NF1 condition suggest that a fate switching event related to NF1 deficiency has occurred in radial glia to produce astrocytes from what otherwise would have been a neural progenitor. This observation in turn both gains credence from and lends credence to the established knowledge that neuronal cell density is reduced in favor of astrocytic cell populations in CNS models of NF1 deletion.

Fate switching in NF1 knockout radial glia such that progeny are more likely to be astrocytic in nature would reasonably decrease the frequency with which CRISPR mediated NF1 negativity was measured via IHC quantification. The contribution of this effect to the evaluation of CRISPR knockout efficiency may be estimated by assuming that pCAG-TDTomato positive astrocytic groupings (which seem to be aclonal) arise from successful deletion of NF1 in radial glia. By this model, the only NF1 negative neurons present in this model would have, by some mechanism, escaped the CRISPR induced fate change.

Data which indicate that radial glia in the NF1 knockout condition have undergone a fate switch from neural to glial progenitor type would support the clinical observation of cognitive deficits in NF1 heterozygous patients. In this case it would seem clear that loss of NF1 promotes atypical differentiation of radial glia towards an astrocytic fate, and that this production of glia occurs at the expense of neuronal cell density.

Conclusions

Although the variables affecting the rate of effective CRISPR mediated knockdown on target genes must still be better characterized, guide RNA sequence, tracrRNA size, and the chromosomal location of the genomic target are all likely to affect the efficiency of any CRISPR/Cas9 editing scheme. With that stated, this work suggests that the IUE CRISPR/Cas9 approach is relevant to the study of neurodevelopmental phenotypes in that loss of function mutations in neural and glial precursors may be readily induced. This approach will be of particular value to the investigation of cortical phenotypes which exhibit defects in neurodevelopment, a high degree of cellular heterogeneity, and loss of heterozygosity in a subpopulation of cells.

With regards to the induced NF1 condition, the CRISPR/Cas9 system was successful in producing a classic NF1 CNS phenotype. It was determined via investigation of proliferative activity in adult animals that this phenotype occurred as the result of an event earlier in neurodevelopment. This phenotype was achieved without the need for the use of a globally heterozygous NF1 animal model, and demonstrated that indeed the NF1 phenotype can arise despite the presence of wild type cells. Although it is well characterized that peripheral NF1 negative glial populations can proliferate and form benign neoplasms as a result of a random loss

of heterozygosity, no clonal expansions resembling tumors were found in the produced NF1 phenotype. Further study should be done to evaluate whether or not a global NF1 heterozygosity alone is sufficient to induce the increased glial density which characterizes this phenotype, or whether the majority of glia which compose the high density population do in fact possess biallelic mutations in NF1. If the latter is found to be the case, further investigation regarding the lack of glioma in this model should be performed, as loss of NF1 heterozygosity leading to complete loss of NF1 expression in peripheral glia is generally regarded as the causative event leading to the formation of neoplasms. Additionally, it is reasonable that an NF1-deficiency mediated proliferation of astrocytes might predispose NF1 heterozygous individuals to certain types of astrocytoma and neurofibroma simply by virtue of the increased cell density present in those individuals. If NF1 heterozygosity alone results in a proliferation of astrocytes during early development, the relative contributions of NF1 deficiency and the increased overall glial population towards the development of astrocytoma and neurofibroma should be better elucidated.

References

Bajenaru, Michaela Livia, et al. "Neurofibromatosis 1 (NF1) heterozygosity results in a cell-autonomous growth advantage for astrocytes." *Glia* 33.4 (2001): 314-323.

Bajenaru, Michaela Livia, et al. "Astrocyte-specific inactivation of the neurofibromatosis 1 gene (NF1) is insufficient for astrocytoma formation."*Molecular and cellular biology* 22.14 (2002): 5100-5113.

Ballas, Nurit, et al. "Non–cell autonomous influence of MeCP2-deficient glia on neuronal dendritic morphology." *Nature neuroscience* 12.3 (2009): 311-317.

Brosens, Lodewijk AA, et al. "Simultaneous Juvenile Polyposis Syndrome and Neurofibromatosis type 1." *Histopathology* (2015).

Brossier, Nicole M., et al. "Classic Ras Proteins Promote Proliferation and Survival via Distinct Phosphoproteome Alterations in Neurofibromin-Null Malignant Peripheral Nerve Sheath Tumor Cells." *Journal of Neuropathology & Experimental Neurology* 74.6 (2015): 568-586.

Carroll, Steven L., and Nancy Ratner. "How does the Schwann cell lineage form tumors in NF1?." *Glia* 56.14 (2008): 1590-1605.

Chen, Fuyi, Albert J. Becker, and Joseph J. LoTurco. "Contribution of Tumor Heterogeneity in a New Animal Model of CNS Tumors." *Molecular cancer research : MCR* 12.5 (2014): 742–753. *PMC*. Web. 25 May 2015.

Chen, Fuyi, Brady J. Maher, and Joseph J. LoTurco. "PiggyBac Transposon-Mediated Cellular Transgenesis in Mammalian Forebrain by In Utero Electroporation." *Cold Spring Harbor Protocols* 2014.7 (2014): pdb-prot073650.

Chen, Fuyi, and Joseph LoTurco. "A Method for Stable Transgenesis of Radial Glia Lineage in Rat Neocortex by *piggyBac* Mediated Transposition." *Journal of neuroscience methods* 207.2 (2012): 172–180. *PMC*. Web. 25 May 2015.

Cong, Le, et al. "Multiplex genome engineering using CRISPR/Cas systems."*Science* 339.6121 (2013): 819-823.

De la Rossa, Andres, and Denis Jabaudon. "In vivo rapid gene delivery into postmitotic neocortical neurons using iontoporation." *Nature protocols* 10.1 (2015): 25-32.

Fields, R. Douglas. "Central Role of Glia in Disease Research." *Neuron glia biology* 6.2 (2010): 91–92. *PMC*. Web. 25 May 2015.

Gutmann, David H., et al. "Optimizing biologically targeted clinical trials for neurofibromatosis." *Expert opinion on investigational drugs* 22.4 (2013): 443-462.

Incontro, Salvatore, et al. "Efficient, Complete Deletion of Synaptic Proteins using CRISPR." *Neuron* 83.5 (2014): 1051-1057.

Jacques, Thomas S., et al. "Combinations of genetic mutations in the adult neural stem cell compartment determine brain tumour phenotypes." *The EMBO journal* 29.1 (2010): 222-235.

Kluwe, Lan, Reinhard Friedrich, and Victor-F. Mautner. "Loss of NF1 allele in schwann cells but not in fibroblasts derived from an NF1-associated neurofibroma." *Genes, Chromosomes and Cancer* 24.3 (1999): 283-285.

LoTurco, Joseph, Jean-Bernard Manent, and Faez Sidiqi. "New and improved tools for in utero electroporation studies of developing cerebral cortex." *Cerebral Cortex* (2009): bhp033.
Mali, Prashant, et al. "RNA-guided human genome engineering via Cas9."*Science* 339.6121 (2013): 823-826.
Meacham, Corbin E., and Sean J. Morrison. "Tumour heterogeneity and cancer cell plasticity." *Nature* 501.7467 (2013): 328-337.
Ratner, Nancy, and Shyra J. Miller. "A RASopathy gene commonly mutated in cancer: the neurofibromatosis type 1 tumour suppressor." *Nature Reviews Cancer* (2015).
Sabatini, Caterina, et al. "Treatment of Neurofibromatosis Type 1." *Current treatment options in neurology* 17.6 (2015): 1-11.
Schaefer, Inga-Marie, and C. D. Fletcher. "Malignant Peripheral Nerve Sheath Tumor (MPNST) Arising in Diffuse-type Neurofibroma: Clinicopathologic Characterization in a Series of 9 Cases." *The American journal of surgical pathology* (2015).
Siddiqi, Faez et al. "Fate Mapping by PiggyBac Transposase Reveals That Neocortical GLAST+ Progenitors Generate More Astrocytes Than Nestin+ Progenitors in Rat Neocortex." *Cerebral Cortex (New York, NY)* 24.2 (2014): 508–520. *PMC*. Web. 25 May 2015.
Sloan, Steven, et al. "Glia as primary drivers of neuropathology in TDP-43 proteinopathies." *PNAS* 10.1073 (2013)
Straub, Christoph, et al. "CRISPR/Cas9-Mediated Gene Knock-Down in Post-Mitotic Neurons." *PloS one* 9.8 (2014): e105584.
Yeh, Tu-Hsueh, et al. "Microarray analyses reveal regional astrocyte heterogeneity with implications for neurofibromatosis type 1 (NF1)-regulated glial proliferation." *Glia* 57.11 (2009): 1239-1249.
Zhang, Shiquen, et al. "5-HT2B receptors are expressed on astrocytes from brain and in culture and are a chronic target for all five conventional 'serotonin-specific reuptake inhibitors'." *Neuron glia biology* 6.02 (2010): 113-125.